Eur Biophys J (2006) 35: 401–409
DOI 10.1007/s00249-006-0047-9

ARTICLE

Hervé Duclohier

Bilayer lipid composition modulates the activity of dermaseptins, polycationic antimicrobial peptides

Received: 21 November 2005 / Revised: 17 January 2006 / Accepted: 30 January 2006 / Published online: 14 February 2006

Abstract The primary targets of defense peptides are plasma membranes, and the induced irreversible depolarization is sufficient to exert antimicrobial activity although secondary modes of action might be at work. Channels or pores underlying membrane permeabilization are usually quite large with single-channel conductances two orders of magnitude higher than those exhibited by physiological channels involved, e.g., in excitability. Accordingly, the ion specificity and selectivity are quite low. Whereas, e.g., peptaibols favor cation transport, polycationic or basic peptides tend to form anion-specific pores. With dermaseptin B2, a 33 residue long and mostly α-helical peptide isolated from the skin of the South American frog *Phyllomedusa bicolor*, we found that the ion specificity of its pores induced in bilayers is modulated by phospholipid-charged headgroups. This suggests mixed lipid–peptide pore lining instead of the more classical barrel–stave model. Macroscopic conductance is nearly voltage independent, and concentration dependence suggests that the pores are mainly formed by dermaseptin tetramers. The two most probable single-channel events are well resolved at 200 and 500 pS (in 150 mM NaCl) with occasional other equally spaced higher or lower levels. In contrast to previous molecular dynamics previsions, this study demonstrates that dermaseptins are able to form pores, although a related analog (B6) failed to induce any significant conductance. Finally, the model of the pore we present accounts for phospholipid headgroups intercalated between peptide helices lining the pore and for one of the most probable single-channel conductance.

H. Duclohier
Institut de Physiologie et de Biologie Cellulaires
(Pôle Biologie Santé), UMR 6187 CNRS-Université de Poitiers,
40 Avenue du Recteur Pineau, 86022, Poitiers, France
E-mail: herve.duclohier@univ-poitiers.fr
Tel.: +33-549-366399
Fax: +33-549-454014

Keywords Pore-forming peptides · Antibiotic resistance · Planar lipid bilayers · Phospholipids · Conductance properties

Introduction

Acquired microbial resistance to classical antibiotics is becoming a serious medical challenge. For about a decade, new antimicrobial, membrane-active peptides have been proposed as an alternative for treating infections. Many recent reviews testify the interest in this fast-growing field (see, e.g., Bulet et al. 2004; Duclohier 2002; Papo and Shai 2003; Boman 2003). Apart from antimicrobiological assays, the bulk of the work devoted to these peptides consists of thorough biophysical investigations of their structure and function. The method of choice in the latter studies is based on conductance properties induced by those membrane-active peptides in planar lipid bilayers as implemented for instance with alamethicin and related peptaibols (for review, see Duclohier and Wroblewski 2001). It is also worth noting that such peptides and especially peptaibols remain interesting models for understanding the structure–function relationships of the more complex physiological ion channels involved, e.g., in membrane excitability (Chugh and Wallace 2001; Duclohier 2003). The range of structures adopted by antimicrobial peptides is large: mostly helical, in, e.g., peptaibols, magainins, gaegurins, cecropins, but also β-sheet or mixed helix-extended structures for instance in human and insect defensins (Selsted and Ouelette 2005; Sahl et al. 2005; Bulet and Stocklin 2005).

At aqueous concentrations relevant for antimicrobial action, the channels or, more properly speaking, the pores underlying membrane permeabilization are usually quite large with single-channel conductances two orders of magnitude higher than those exhibited by in situ physiological channels involved in excitability. Accordingly, the ion specificity (between cations and anions) is quite low. As for ion selectivity (within a

cation or anion series), it is most often in favor of cations with, e.g., peptaibols whereas polycationic peptides such as magainins tend to form anion-specific pores (Duclohier et al. 1989). An interesting feature was recently found with dermaseptin B2, the most abundant peptide isolated from the skin of the South American frog *Phyllomedusa bicolor* (Daly et al. 1992). This 33 residue long and mostly α-helical peptide whose aminoacid sequence (one-letter code) is shown in Fig. 1 together with its helical (or Edmunson) wheel exhibits antimicrobial activity (Fleury et al. 1998) as well as other members of the dermaseptin family (Amar et al. 1998). As it was previously found with many other antimicrobial peptides that their activity was correlated with transmembrane pores formation and moreover with pore sizes (Béven et al. 1999), toward understanding dermaseptin molecular mode of action, we investigated its membrane permeabilization properties using the planar lipid bilayers technique. The main results reported here are that, contrary to expectations issued from molecular modeling and other considerations, dermaseptin B2 does form well resolved channel events and the pores' ion specificity was modulated by membrane lipid-charged headgroup. This can be best and simply explained by the formation of mixed lipid–peptide pore lining and a toroidal model instead of the more classical barrel–stave layout accounting for peptaibols pores.

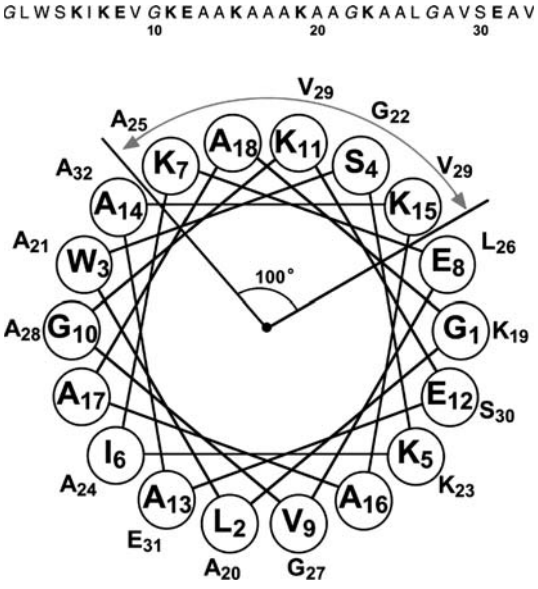

Fig. 1 Aminoacid sequence (one-letter code) and helical wheel of dermaseptin B2. In the sequence, electrically charged residues are in *bold* and the potential 'helix breaker' G is in *italics*. Position markers are given *below* the sequence. The helical Edmunson wheel (projection of all residues on a plane, assuming a straight helix) is shown *below* the sequence with the first 18 residues (those most likely to be embedded in the bilayer) *circled*. The *circular ark terminated by arrows* delineate the most probable hydrophilic sector making an angle of 100°

Materials and methods

Dermaseptin B2, the most abundant peptide isolated and purified from the skin of the South American frog *Phyllomedusa bicolour*, was kindly supplied by P. Nicolas (Université de Paris VII, Jussieu, France). The lipids used to form planar bilayers were L-α-phosphatidylcholine, L-α-phosphatidylethanolamine, L-α-phosphatidylserine and cholesterol, all obtained from SIGMA-ALDRICH (St Louis, MO, USA), as well as hexadecane and hexane (spectroscopic grade). In some conductance experiments, total membrane lipids extracted from *Spiroplasma citri* (Wroblewski et al. 1978) were also used for bilayer formation. These lipids are later abbreviated as PC, PE, PS, Chol and Spiro, respectively.

Conductance on planar lipid bilayers

Conductance properties induced by Dermaseptin B2 in planar lipid bilayers were assayed as previously described (Duclohier et al. 1989). Briefly, macroscopic conductances resulting from the activity of hundreds or thousands of channels were recorded in virtually solvent-free bilayers (Montal and Mueller 1972) doped with peptide and exposed to slow voltage ramps (typically 1 min per cycle over a ±150 mV range). The bilayer was made by folding two lipid monolayers over a 150–200 μm hole in a PTFE (GOODFELLOW, Huntingdon, UK) film sandwiched between two half glass cells. The hole had been previously pretreated with a few microliters of a 4% hexadecane solution in hexane. The electrolyte on both sides of the bilayer was either 1 M or 150 mM NaCl, 10 mM Hepes (pH 7.4) except when elsewhere noted. Voltage was delivered via an Ag/AgCl electrode on the *cis* side of the bilayer (the *cis* side refers to the side of peptide addition and the electrically positive side of the bilayer). Currents are measured via a second electrode in the *trans* side connected to an amplifier and current–voltage converter.

For recordings of single-channel activity, bilayers were made at the tip of patch pipettes as described previously (Hanke et al. 1984), and a standard patch-clamp apparatus (from DAGAN Corp., Minneapolis, MN, USA) was used. Here, the peptide was added in the external bath and voltage commands were delivered and currents measured via an electrode inside the pipette. Voltage conditioning, acquisition and analysis of current recordings were carried out with the SES software (Strathclyde Electrophysiology Softwares) kindly supplied by Dr. J. Dempster (Strathclyde University, Glasgow, UK). The composition of the bilayer-forming lipids in both macroscopic and single-channel conductance configurations are given within the text and in the figure legends.

Results

Macroscopic conductance: voltage independence and modulation of ion specificity with bilayer lipid composition

Macroscopic current–voltage (*I–V*) curves, shown in Fig. 2, were recorded from negatively charged lipid bilayers containing cholesterol, exposed to a micromolar concentration of dermaseptin B2 and submitted to slow voltage ramps (2 mV/s). These quasi-linear *I–V* curves indicate an ohmic behavior, i.e., a voltage-independent conductance. Curve a was recorded in symmetrical ionic conditions (150 mM NaCl on both sides of the bilayer) whereas the imposition of an ion gradient (550 mM NaCl in the *trans* side, keeping 150 mM in the *cis* side) resulted in a significant shift of the reversal potential (E_{rev}) corrected for liquid junction potential checked at the beginning and end of the experiments. The ratio of sodium and chloride ions permeabilities (P_{Na}/P_{Cl}) can be estimated by applying a simplified form of the Goldman–Hodgkin–Katz (Goldman 1943; Hodgkin and Katz 1949) equation:

$$E_{rev} = [RT/F]\ln[(P_{Na}[Na]_t + P_{Cl}[Cl]_c)/(P_{Na}[Na]_c + P_{Cl}[Cl]_t)],$$

where R, T, F are the universal gas constant, the absolute temperature and the Faraday constant, respectively. P_{Na} and P_{Cl} are potassium and chloride permeabilities whereas $[Na]_t$ and $[Na]_c$ are the sodium concentrations in *trans* and *cis* compartments, respectively. The same notation applies for Cl^-.

With neutral bilayers (PC/PE, 1/1), an anion specificity P_{Cl}/P_{Na} of 7 on average ($N=4$ experiments) was found whereas this specificity was nearly insignificant (1.4) with negatively charged bilayers (PC/PE/Chol/PS, 2.8/2.8/2.4/2).

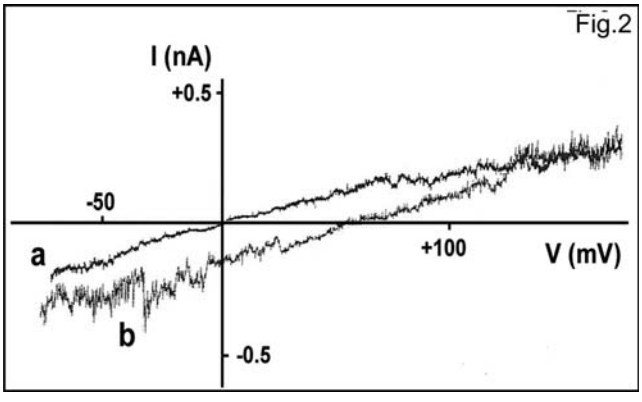

Fig. 2 Macroscopic current–voltage (*I–V*) plots recorded from negatively charged lipid bilayers containing cholesterol (PC/PE/PS/Chol, 2/2/3/3) and exposed to 10^{-6} M DS-B2 (*cis* side) and submitted to slow voltage ramp (5 mV/s). *Curve a* shows the response in symmetrical 150 mM NaCl whereas *curve b* was obtained after an NaCl gradient (0.15 M/0.55 M, *cis*/*trans*). Room temperature: 22°C

Concentration dependence and oligomerization state

Besides voltage-dependence (or independence) characterization, another investigation at the macroscopic current level usually carried with pore-forming peptides is the concentration dependence of *I–V* curves upon increasing the amount of peptide on both sides of the bilayer. Figure 3 shows an example of such an experiment with dermaseptin B2. The bilayer submitted to voltage linear ramps (lower trace) developed the currents shown in the upper part of the figure. The smaller current is strictly ohmic whereas the higher concentration tends to develop a slight voltage dependence (upward curvature) for the rising phase. The application of the equation

$$G_j/G_i = (C_j/C_i)N,$$

where G_j and G_i are the conductances associated with the peptide concentrations C_j and C_i and N the apparent mean number of peptide monomers per conducting transmembrane aggregate (Eisenberg et al. 1973; Hall et al. 1984), yields a mean value (average of three experiments) for $N=3.7$ (rounded as $N=4$), with extreme values 3.2 and 4.3, taking into account errors in measuring the chord or slope conductances.

Single-channel conductances: kinetics depends on bilayer lipid composition

The investigation began with standard conditions, i.e., using neutral planar lipid bilayers (PC/PE, 1/1) bathed on both sides with 1 M NaCl. The pattern of activity and single-channel levels was dependent on both the peptide concentration and time after its addition (always *cis* side). The results of a representative experiment (out of $N=5$) are summarized in Fig. 4 which shows two main, most probable and well-resolved events induced

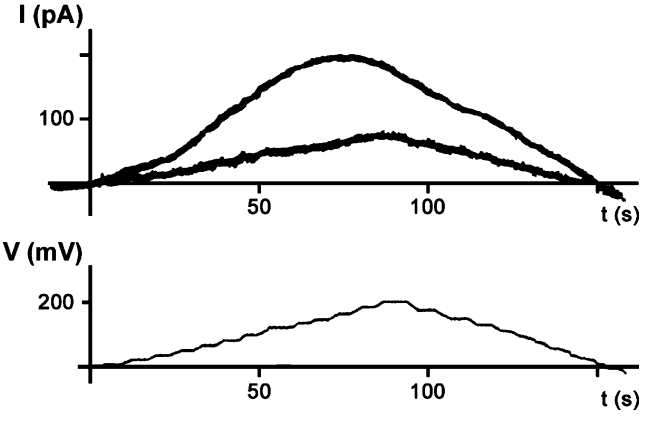

Fig. 3 Concentration dependence and oligomerization state. The bilayer was formed from neutral lipids (PC/PE, 1/1) bathed on both sides by 150 mM NaCl. The peptide concentrations associated with the lower and upper current traces (*upper part* of the figure) are 0.7×10^{-7} and 10^{-6} M, respectively

by peptide concentrations in the 10^{-6}–10^{-7} M range. Note the progressive recruitment of 500 pS channels in the continuous recording shown in part b of Fig. 4.

In bilayers incorporating charged phospholipid headgroups (PC/PE/PS, 4/4/2, w/w), very fast and hardly resolved single-channel events were observed. Better-resolved single channels were recorded after the addition of cholesterol as in PC/PE/PS/Chol (2/2/3/3) bilayers as shown in Fig. 5. These bilayers were assayed in an attempt to mimic the natural target membranes since extracted *Spiroplasma* membrane lipids failed to produce stable bilayers. In symmetrical 150 mM NaCl, the single-channel current fluctuations are quite rapid, although still resolved, as shown in Fig. 5a (enlarged inset). The amplitude histogram (Fig. 5b) also points to a more complex distribution of single-channel levels than in neutral bilayers (see above and Fig. 4): a minor level at 65 pS (two equally spaced transitions) and another one at about 170 pS. These levels are all nearly equally probable (around 2%). Single-channel data in the various ionic conditions and bilayer lipid compositions are summarized in Table 1. Errors were mainly due to the width of the amplitude histogram peaks.

Assays of a closely related analog

Another peptide of the same family (dermaseptin B6) was also tested. It is only 24 residues long instead of 33 for B2 and presents three lysines instead of six. This results, for the helical wheel, in a hydrophilic sector very much reduced in comparison with dermaseptin B2. In the macroscopic conductance configuration, large concentrations (up to 1.5 μM, *cis* side) of B6 failed to induce any significant conductance. Out of three different experiments at six voltages (50–190 mV), the average ohmic or leak conductance was 49 ± 3 pS in POPC/DOPE (1:1) bathed on both sides with 150 mM NaCl, that is barely above the bare bilayer background conductance.

Discussion

The data reported here can be summarized as follows: (1) macroscopic conductance is nearly voltage independent, and concentration dependence suggests that dermaseptin pores are mainly tetrameric; (2) the ion specificity of dermaseptin B2 pores induced in bilayers is modulated by lipid-charged headgroups; and (3) the most probable single-channel events are well resolved at 200 and 500 pS (in 1 M NaCl) in neutral bilayers with occasional other higher or lower levels in negatively charged bilayers. Thus, contrary to previous molecular dynamics previsions (La Rocca et al. 1999), our study demonstrates that dermaseptins are able to form channels. In the future and in order to better mimic natural membrane targets, we plan to form asymmetrical planar bilayers with polysaccharides at the outer bilayer leaflet. In any case, the criteria put forward in a short paper (Homblé et al. 1998) for a peptide, whether antimicrobial or not, to induce 'real' discrete channels and not erratic membrane disorganization are clearly met here with dermaseptin B2. A detergent-like mode of action as recently put forward for magainin (Bechinger et al. 2005) is apparently ruled out here, at the assayed peptide concentrations, since it would shortly lead to irreversible leakage and not to single-channel events. It would be interesting to test in planar lipid bilayers another dermaseptin analog, dermaseptin S9, very recently studied and which differs significantly since its sequence (24 aminoacid long) shows a central hydrophobic core

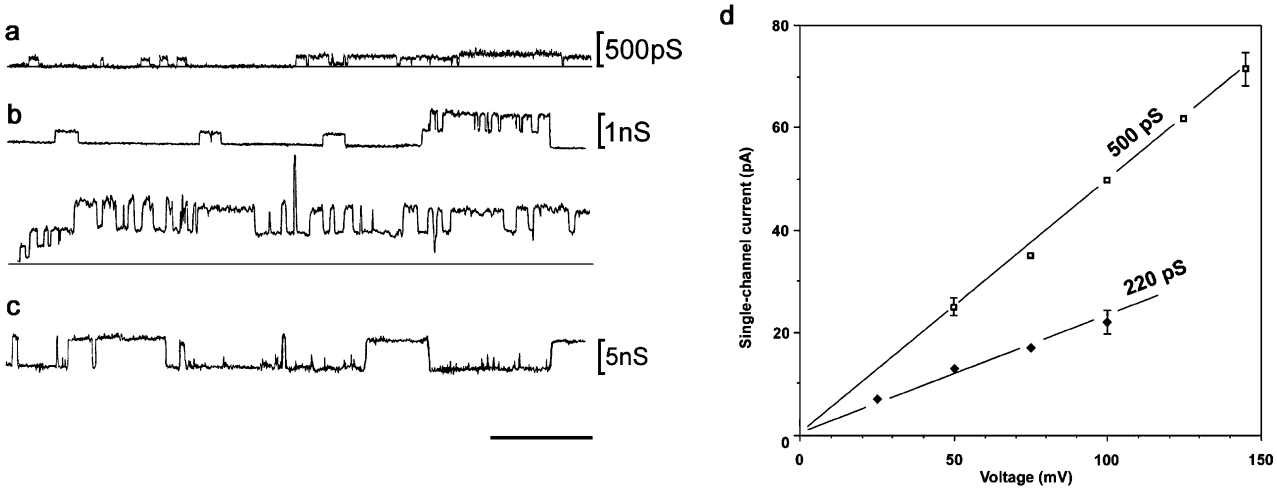

Fig. 4 Single-channel events recorded in PE/PC bilayers symmetrically bathed by 1 M NaCl and at room temperature. Traces lasting 600 ms at three different applied voltages and DS-B2 aqueous concentrations (*cis* side): 25 mV and 2.5×10^{-7} M (**a**); 50 mV and 5×10^{-7} M (**b**); 100 mV and 10^{-6} M (**c**), respectively. *Openings* are upward deflections and *thin lines* represent closed levels. *Horizontal scale bar* is 100 ms for traces **a** and **c** and 200 ms for trace **b**. *Vertical scale bar* is 25 pA for trace **a**, 100 pA for trace **b** and 500 pA for **c**. **d** Single-channel current versus voltage plot for the two most probable levels

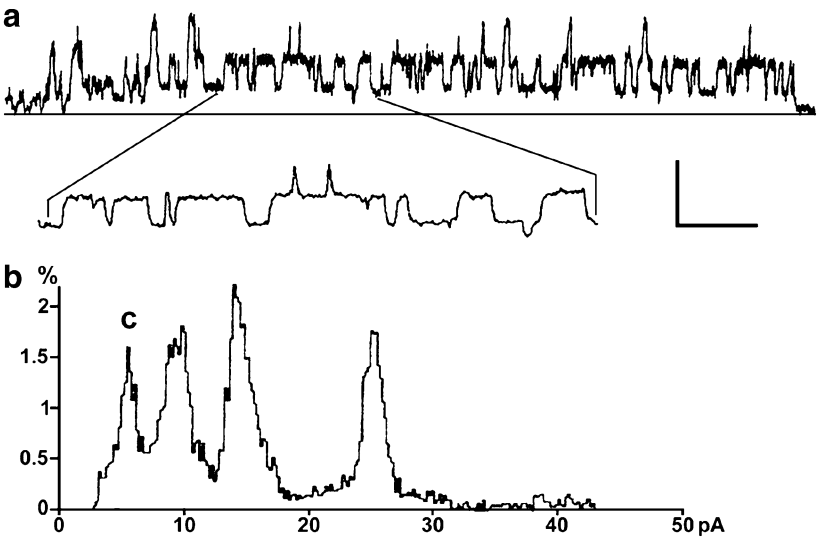

Fig. 5 Single-channel traces in negatively charged bilayers with cholesterol. Trace **a** is from a PC/PE/PS/Chol (2/2/3/3) bilayer in symmetrical 150 mM NaCl and with 10^{-6} M DS-B2 (*cis* side) at an applied voltage of 75 mV. The *inset* shows a selected portion on a four-times enlarged time-base. *Horizontal* and *vertical scale bars* are for 1 s and 20 pA, respectively. *Openings* are upward deflections, the *thin line* representing zero current level. The corresponding amplitude histogram is shown in **b**, with the closed level indicated as *C* and conductance levels of 65 and 170 pS

Table 1 Summary of single-channel conductances (with SEM) in planar bilayers of different lipid compositions

Planar bilayer composition	Channel events	Unit conductance (pS)	Open lifetime (ms)
PC/PE (1/1)	Yes	*200* ± 18, 500 ± 22	50
PC/PE/Chol (3.5/3.5/3)	No	–	–
PC/PE/PS (4/4/2)	Yes	140 ± 5, *200* ± 6, 270 ± 9	10
PC/PE/PS/Chol (2/2/3/3)	Yes	65 ± 2, *170* ± 4	200
PC/PE/Spiro (4/4/2)	Poorly resolved	*200* ± 5	–

The range of peptide concentration assayed is 10^{-7}–10^{-6} M (*cis* side) and the electrolytic solution on both sides is: 150 mM NaCl, 5 mM Hepes, pH 7. Room T ~21°C. Main (most probable) levels are italicized

and cationic termini (Lequin et al. 2006). The Edmunson wheel points to a much larger hydrophilic sector than dermaseptin B2, although many neutral residues are interspersed between charged residues. The authors stated that " ... spatial segregation of hydrophobic and hydrophilic/charged residues on opposing faces along the long axis of a helix is not essential for the antimicrobial activity of cationic α-helical peptides" (Lequin et al. 2006).

The main mechanisms of action of membrane-active peptides are schematized in Fig. 6 (kindly provided by Professor Yechiel Shai). The prototype of peptides forming transmembrane helices and aggregating in a 'barrel–stave' (on the left in Fig. 6) is alamethicin. This model was based on alamethicin crystal structure (Fox and Richards 1982), and this antimicrobial peptaibol also results in membrane excitability (Mueller and Rudin 1968; Duclohier and Spach 2001), voltage-dependent macroscopic current (Hall et al. 1984) and yields well-defined single-channel levels whose kinetics depends upon the lipid composition of the bilayer (Keller et al. 1993). Instead of equal increments between these levels as would be the case with, e.g., gramicidin and even with dermaseptin B2, as shown in the present work, the increments displayed by alamethicin are in a geometrical progression reflecting the uptake and release of individual helical monomers in the barrel–stave (Hanke and Boheim 1980).

In the case of dermaseptin B2 whose space-filling model of the helix based on a structural analysis (Lequin et al. 2003) is shown in Fig. 7, kindly provided by Dr. Maria-Antonietta Castiglione-Morelli (Castiglione-Morelli et al. 2005), the modulation of ion specificity with bilayer composition strongly suggests that the mechanism of action is more likely to obey the 'carpet' types of models (Oren and Shai 1998) shown on the right of Fig. 6, and specifically the toroidal pores (Yang et al. 2001; Lee et al. 2004). Note that the 'perturbation energy' due to transmembrane-inserted peptides and pores is smaller than with the same absorbed peptides on the bilayer surface (Zemel et al. 2005). Dermaseptin pores would be lined both by the lysine positively charged side chains of the peptide hydrophilic sector and by intercalated phospholipid headgroups. If the latter are neutral as in PC and PE, it is conceivable that the anion flux favored by lysines will be higher than with PS-containing bilayers where the negatively charged headgroups will electrostatically impede Cl^- permeation through the lumen.

A model of the channel with four helices and negatively charged and neutral phospholipid headgroups intercalated between the peptide helices lining the pore is shown in Fig. 8. The helix and headgroups' approximative diameters are 14 Å (see http://www.cryst.bbk.ac.uk) and 7 Å, respectively, leaving an aqueous lumen with a diameter of about 14 Å. Applying the following equation (Hille 1992):

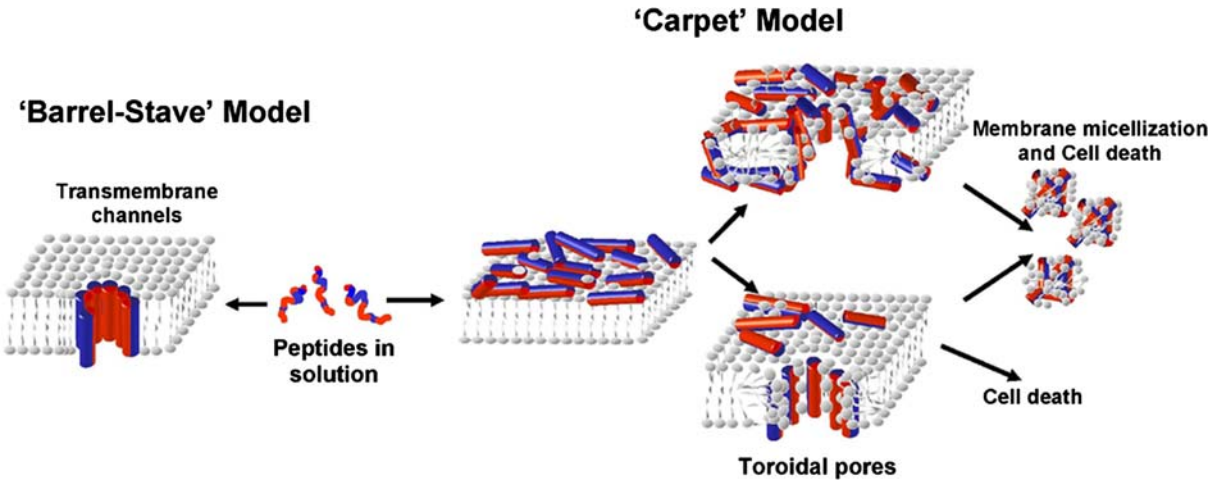

Fig. 6 Two major different mechanisms of membrane lysis by membrane permeating peptides. Peptides can either form transmembrane pores via the 'barrel–stave' mechanism. This results in membrane depolarization followed by cell death. Alternatively, peptides bind in the first step mainly by electrostatic interactions and align parallel to the outer membrane surface (step one) and cover it in a 'carpet-like' manner (Papo and Shai 2003; Oren and Shai 1998). When a threshold concentration of peptides has been reached (the second step), the peptides disrupt the membrane, which is often followed by membrane disintegration and micellization. Specific long peptides can form, described as, 'toroidal' pore (Lee et al. 2004). Further peptide accumulation unto the cell membrane or bilayer leads to membrane disruption and micellization

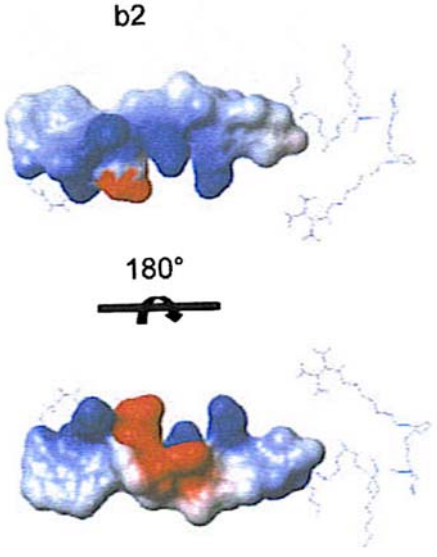

Fig. 7 Dermaseptin B2 helix. Contact surface *colored* according to the electrostatic potential based on the structure found in TFE/water (Lequin et al. 2003). For details, see Castiglione-Morelli et al. 2005. (Courtesy of Dr. Maria Antonietta Castiglione)

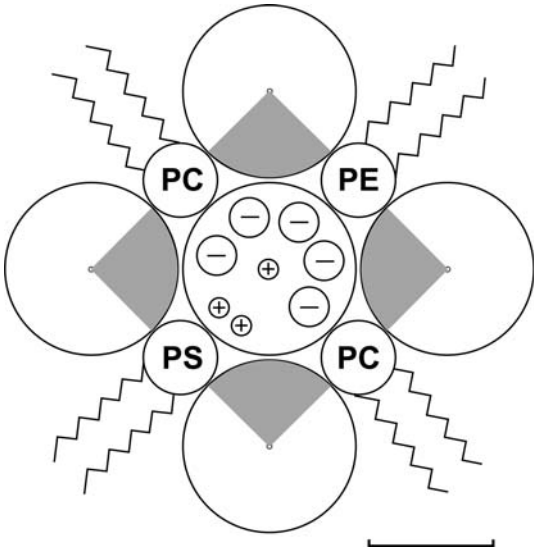

Fig. 8 Top view of a model of a tetrameric dermaseptin pore with intercalated negatively charged and neutral phospholipid headgroups. Molecules are drawn to scale with helices and headgroups diameters of 14 and 7 Å, respectively. Hydrated sodium and chloride ions (Pauling radii of 0.95 and 1.81 Å, respectively) tend to accumulate near positively charged sectors of the peptide helices and the phosphatidylserine headgroups. Three Na^+ and five Cl^- are represented to account for the experimentally found P_{Na}/P_{Cl} of 1.4. This structure is embedded in the surrounding lipid matrix (not shown here). The calibration at the *bottom right* represents 10 Å

$$R_{pore} = 1/G_{pore} = \rho L/\pi r^2,$$

with R the resistance (in ohms), ρ the resistivity of the conducting medium ($\rho = 100\ \Omega$ cm for a 150 mM NaCl solution), r the diameter of the pore lumen and L its length set at 30 Å (bilayer thickness), yields a conductance of about 500 pS, i.e., one of the two most probable single-channel conductance found in experiments, only if a single phospholipid headgroup is intercalated between two helices. In the future, it might prove worthwhile to use crown ethers as molecular probes to more precisely calibrate the pore diameter as implemented recently with the α-hemolysin channel (Krasilnikov et al. 2005).

By analogy with another class of cationic peptides whose interactions in a membrane-mimicking environment and cellular uptake efficiency were very recently compared (Balayssac et al. 2006), it may be inferred that

the overall translocation and internalization of dermaseptin B2 is weak or restricted. In the above-mentioned study, the structures in SDS micelles of four peptides corresponding to the third helix sequence of the *Drosophila* Antennapedia homeodomain were studied by NMR spectroscopy and the depth of insertion was investigated using Mn^{2+} as a paramagnetic probe (Balayssac et al. 2006). As for cellular uptake, it was quantified by a recently developed method based on MALDI-TOF MS (matrix-assisted laser desorption ionization-time-of-flight mass spectrometry). The peptide with highest uptake efficiency (Knotted-1) was found to be the least deeply inserted within the micelle, presumably because of a large density of positively charged residues near the C terminus, especially a $R^+K^+R^+$ cluster (Balayssac et al. 2006). Dermaseptin B2 sequence and distribution of charged residues rather resembles another peptide of these series, i.e., Engrailed-2 which presents about the same number of arginines and lysines but not clustered. The central portion of the latter peptide is more deeply inserted than Knotted-1 and its internalization or cellular uptake is smaller. In addition, the authors suggest that the presence of an acidic residue, as in the Hox peptide (and incidentally as in dermaseptin B2), may be detrimental for cellular uptake. Note that as the concentration increases (high peptide/lipid ratios), peptide secondary structure may shift from α-helical to β-sheet and causes greater membrane perturbation (Magzoub et al. 2001; Persson et al. 2001).

In addition to pore or channel formation and membrane permeabilization, other modes of action of antimicrobial peptides may play a role in killing bacteria. In particular, alamethicin uncouples mitochondrial oxidative phosphorylation (Mathew et al. 1981), facilitates mitochondrial cytochrome oxidase respiration (Shaughnessy and Nicholls 1985), unmasks the latent activity of Ca^{2+}-stimulated ATPase (Seppet and Dhalla 1989) and of the β-adrenergic receptor-coupled adenylate cyclase (Jones et al. 1980). However, these actions appear secondary or as a consequence of membrane permeabilization (Krasnikov et al. 2005). Some antimicrobial peptides, such as lantibiotics secreted by Gram-positive organisms and much more potent than traditional antibiotics such as penicillin, exert their action from the outside, i.e., on the bacterial envelope or wall. Indeed, lantibiotics bind to a special class of membrane lipids, lipid II, which is a prenyl-chain donor of the peptidoglycan building blocks. Antibiotics binding lead to an inhibition of peptidoglycan biosynthesis and thus of the cell wall, essential for bacterial survival (Lohner and Blondelle 2005). Molecular oligomerization of some antimicrobial peptides, as distinctin, in aqueous solution can play a role in resistance to degradation by proteases, without affecting hemolytic and channel or pore formation (Raimondo et al. 2005). A well-known and rare example of peptide that crosses membranes or lipid bilayers without significantly forming pores and without inducing lipid flip–flop is buforin 2 extracted from the stomach of the Asian toad *Bufo bufo*. This 21 residue long and linear peptide transiently disrupts membranes and presumably acts on cytoplasmic targets (Kobayashi et al. 2004). The only proline towards the middle of the sequence (at position 11) was found to play a key role in this behavior (Park et al. 2000). The mode of action exhibited by buforin is unlikely to apply in the case of dermaseptins since they permeabilize bilayers and membranes through channel or pore formation and besides there is no proline in the sequence of dermaseptin B2. As a rule, peptide translocation across bilayers is found to be higher for β-sheet peptide (such as polyphemusin), intermediate for β-α-helical peptides and low for extended peptides (such as indolicidin) (Zhang et al. 2001). It is also important to note that the mechanism of action is strongly dependent on the peptide concentration or peptide/lipid ratio. When present in the cytoplasm, some cationic peptides are thought to bind to DNA, RNA and to inhibit the biosynthesis of these compounds and/or cellular proteins (Yonezawa et al. 1992). Specific enzymatic targets have been identified for, e.g., a proline-rich insect peptide (pyrrhocoricin) which was shown to bind a heat shock protein and inhibit chaperone-assisted protein folding (Kragol et al. 2001). Finally, for these peptides, the loss of viability is much slower than with membrane-active peptides which exert their effects within minutes (Powers and Hancock 2003).

Finally, antimicrobial or defense peptides play a role in innate immunity and exhibit antiproliferative activity, especially against breast cancer and leukemia cells (Wong and Ng 2005). This anti-carcinogenic potency was recognized a long time ago, e.g., cationic peptides MCP-1 and -2 isolated from rabbit alveolar macrophages were active against two tumor cell lines of murine lymphosarcoma origin but not against the normal cell lines tested (Sheu et al. 1985). A designed synthetic peptide was shown to be efficient in the treatment of solid tumors by local injection and it was suggested it could be used as an adjuvant therapy in conjunction with radiotherapy, chemotherapy, immunotherapy and surgery (Mai et al. 2001). In addition to pore forming and membrane micellization (at higher peptide/lipid molar ratios), magainin was also shown to trigger apoptosis of human promyelocytic leukemia HL-60 cells (Cruz-Chamorro et al. 2005). In addition to antiproliferative activity, a few peptides such as Sesquin, isolated from ground beans, exhibit some inhibitory activity against human immunodeficiency virus-type 1 reverse transcriptase (Wong and Ng 2005). This potential new clinical use of host defense or antimicrobial peptides in cancer treatment has been recently reviewed by Papo and Shai (2005).

Faced with acquired resistance to classical antibiotics in the clinical treatment of infections, numerous pore-forming peptides are currently in development as antimicrobial agents with potential application as antitumorigenic agents and biosensors (Panchal et al. 2002).

Efforts are also being made to render these molecules cell-targetable and regulable cell-killing agents. Finally, interplay and synergies between antimicrobial effectors (Rosenberger et al. 2004) together with ongoing studies of natural and synthetic peptides offer great hope for the design of new and specific antimicrobials (Yount and Yeaman 2004).

Acknowledgements I thank Henri Wroblewski (Université de Rennes I, France) for providing space in his laboratory, supplying peptides and for critical comments. I also warmly thank Yechiel Shai (The Weizmann Institute of Science, Rehovot, Israel) and Maria-Antonietta Castiglione-Morelli (Universita della Basilicata, Potenza, Italy) for their kind permission to reproduce their Figs. 6 and 7, respectively from Papo and Shai (2003) and Castiglione-Morelli et al. (2005). Finally, many thanks are due to J.-P. Poindessault (UMR 6187 CNRS-Université de Poitiers) for his friendly help in preparing the figures.

References

Amar B, Perianin A, Mor A, Sarfati G, Tissot M, Nicolas P, Giroud JP, Roch-Arweiller M (1998) Dermaseptin, a peptide antibiotic, stimulates microbicidal activities of poymorphonuclear leukocytes. Biochem Biophys Res Commun 247:870–875

Balayssac S, Burlina F, Convert O, Bolbach G, Chassaing G, Lequin O (2006) Comparison of penetratin and other homeodomain-derived cell-penetrating peptides: interaction in a membrane-mimicking environment and cellular uptake efficiency. Biochemistry 45(5):1408–1420

Bechinger B, Aisenbrey C, Bertani P (2005) Detergent-like properties of magainin antibiotic peptides: a ^{31}P solid-state NMR spectroscopy study. Biochim Biophys Acta 1712:101–108

Béven L, Helluin O, Duclohier H, Wroblewski H (1999) Correlation between antibacterial activity and pore sizes of two classes of voltage-dependent channel-forming peptides. Biochim Biophys Acta 1421:53–63

Boman HG (2003) Antibacterial peptides: basic facts and emerging concepts. J Intern Med 254:197–215

Bulet P, Stocklin R (2005) Insect antimicrobial peptides: structures, properties and gene regulation. Protein Pept Lett 12:3–11

Bulet P, Stocklin R, Menin L (2004) Antimicrobial peptides: from invertebrates to vertebrates. Immunol Rev 198:169–184

Castiglione-Morelli MA, Cristinziano P, Pepe A, Temussi PA (2005) Conformation–activity relationship of a novel peptide antibiotic: structural characterization of dermaseptin DS 01 in media that mimic the membrane environment. Biopolymers 47:688–696

Chugh JK, Wallace BA (2001) Peptaibols: models for ion channels. Biochem Soc Trans 29:565–570

Cruz-Chamorro L, Puertollano MA, Puertollano E, de Cienfuegos GA, de Pablo MA (2005) In vitro biological activities of magainin alone or in combination with nisin. Peptides (in press)

Daly JW, Caceres J, Moni RW, Gusovsky F, Moos M Jr, Seamon KB, Milton K, Myers CW (1992) Frog secretions and hunting magic in the upper Amazon: identification of a peptide that interacts with an adenosine receptor. Proc Natl Acad Sci USA 89:10960–10963

Duclohier H (2002) How do channel- and pore-forming helical peptides interact with lipid membranes and does this account for their antimicrobial activity? Mini Rev Med Chem 2:331–342

Duclohier H (2003) Insights into ion channels from peptides in planar lipid bilayers. In: Tien HT, Ottova-Leitmannova A (eds) Planar lipid bilayers (BLMs) and their applications. Elsevier, Amsterdam, pp 89–604

Duclohier H, Spach G (2001) Artificial membrane excitability revisited and implications for the gating of voltage-dependent ion channels. Gen Physiol Biophys 20:361–374

Duclohier H, Wroblewski H (2001) Voltage-dependent pore formation and antimicrobial activity by alamethicin and analogues. J Membr Biol 184:1–12

Duclohier H, Molle G, Spach G (1989) The antimicrobial peptide magainin I from *Xenopus* skin forms anion-permeable channels in planar lipid bilayers. Biophys J 56:175–188

Eisenberg M, Hall JE, Mead CA (1973) The nature of the voltage-dependent conductance induced by alamethicin in black lipid membranes. J Membr Biol 14:143–176

Fleury Y, Vouille V, Beven L, Amiche M, Wroblewski H, Delfour A, Nicolas P (1998) Synthesis, antimicrobial activity and gene structure of a novel member of the dermaseptin B family. Biochim Biophys Acta 1396:228–236

Fox RO, Richards FM (1982) A voltage-gated ion channel inferred from the crystal structure of alamethicin at 1.5 A resolution. Nature 25:325–330

Goldman DE (1943) Potential, impedance, and rectification in membranes. J Gen Physiol 27:37–60

Hall JE, Vodyanoy I, Balasubramanian TM, Marshall GR (1984) Alamethicin: a rich model for channel behavior. Biophys J 45:233–247

Hanke W, Boheim G (1980) The lowest conductance state of the alamethicin pore. Biochim Biophys Acta 596:456–462

Hanke W, Methfessel C, Wilmsen U, Boheim G (1984) Ion channel reconstitution into planar lipid bilayers on glass pipettes. Biochem Bioenerg J 12:329–339

Hille B (1992) Ionic channels of excitable membranes, 2nd edn. Chapter 11: Elementary properties of pores. Sinauer Associates, Sunderland, pp 291–314

Hodgkin AL, Katz B (1949) The effect of sodium ions on the electrical activity of the giant axon of the squid. J Physiol 108:37–77

Homblé F, Cabiaux V, Ruysschaert J-M (1998) Channel or channel-like activity associated with pore-forming proteins or peptides. Mol Microbiol 27:1261–1263

Jones LR, Maddock SW, Besch HR Jr (1980) Unmasking effect of alamethicin on the (Na^+-K^+)-ATPase, beta-adrenergic receptor-coupled adenylate cyclase, and cAMP-dependent protein kinase activities of cardiac sarcolemmal vesicles. J Biol Chem 255:9971–9980

Keller SL, Bezrukov SM, Gruner SM, Tate MW, Vodyanoy I, Parsegian VA (1993) Probability of alamethicin conductance states varies with nonlamellar tendency of bilayer phospholipids. Biophys J 65:23–27

Kobayashi S, Chikushi A, Tougu S, Imura Y, Yano Y, Matsuzaki K (2004) Membrane translocation mechanism of the antimicrobial peptide buforin 2. Biochem 43:15610–15616

Kragol G, Lovas S, Varadi G, Condie BA, Hoffmann R (2001) The antibacterial peptide pyrrhocoricin inhibits the ATPase actions of DnaK and prevents chaperone-assisted protein folding. Biochemistry 40:3016–3026

Krasilnikov OV, Merzlyak PG, Yuldasheva LN, Capistrano MF (2005) Protein electrostriction: a possibility of elastic deformation of the α-hemolysin channel by the applied field. Eur Biophys J 34:997–1006

Krasnikov BF, Zorov DB, Antonenko YN, Zaspa AA, Kulikov IV, Kristal BS, Cooper AJL, Brown AM (2005) Comparative kinetic analysis reveals that inducer-specific ion release precedes the mitochondrial permeability transition. Biochim Biophys Acta 1708:375–392

La Rocca P, Shai Y, Sansom MS (1999) Peptide-bilayer interactions: simulations of dermaseptin B, an antimicrobial peptide. Biophys Chem 76:145–169

Lee M-T, Chen F-Y, Huang HW (2004) Energetics of pore formation induced by membrane active peptides. Biochemistry 43:3590–3599

Lequin O, Bruston F, Convert O, Chassaing G, Nicolas P (2003) Helical structure of dermaseptin B2 in a membrane-mimetic environment. Biochemistry 42:10311–10323

Lequin O, Ladram A, Chabbert L, Bruston F, Convert O, Vanhoye D, Chassaing G, Nicolas P, Amiche M (2006) Dermaseptin S9, an a-helical antimicrobial peptide with a hydrophobic core and cationic termini. Biochemistry 45:468–480

Lohner K, Blondelle SE (2005) Molecular mechanisms of membrane perturbation by antimicrobial peptides and the use of biophysical studies in the design of novel peptide antibiotics. Comb Chem High Throughput Screen 8:241–256

Magzoub M, Kilk K, Eriksson LEG, Langel U, Gräslund A (2001) Interaction and structure induction of cell-penetrating peptides in the presence of phospholipid vesicles. Biochim Biophys Acta 1512:77–89

Mai JC, Mi Z, Kim SH, Ng B, Robbins PD (2001) A proapoptotic peptide for the treatment of solid tumors. Cancer Res 61:7709–7712

Mathew MK, Nagaraj R, Balaram P (1981) Alamethicin and synthetic peptide fragments as uncouplers of mitochondrial oxidative phosphorylation. Effect of chain length and charge. Biochem Biophys Res Commun 98:548–555

Montal M, Mueller P (1972) Formation of bimolecular membranes from monolayers and study of their electrical properties. Proc Natl Acad Sci USA 69:3561–3566

Mueller P, Rudin DO (1968) Action potentials induced in bimolecular lipid membranes. Nature 217:713–719

Oren Z, Shai Y (1998) Mode of action of linear amphipathic alpha-helical antimicrobial peptides. Biopolymers 47:451–463

Panchal RG, Smart ML, Bowser DN, Williams DA, Petrou S (2002) Pore-forming proteins and their application in biotechnology. Curr Pharm Biotechnol 3:99–115

Papo N, Shai Y (2003) Can we predict biological activity of antimicrobial peptides from their interactions with model phospholipid membranes. Peptides 24:1693–1703

Papo N, Shai Y (2005) Host defense peptides as new weapons in cancer treatment. Cell Mol Life Sci 62:784–790

Park CB, Yi KS, Matsuzaki K, Kim MS, Kim SC (2000) Structure–activity analysis of buforin II, a histone H2A-derived antimicrobial peptide: the proline hinge is responsible for the cell-penetrating ability of buforin II. Proc Natl Acad Sci USA 97:3245–8250

Persson D, Thoren PE, Norden B (2001) Penetratin-induced aggregation and subsequent dissociation of negatively-charged phospholipid vesicles. FEBS Lett 505:307–312

Powers JP, Hancock REW (2003) The relationship between peptide structure and antibacterial activity. Peptides 24:1681–1691

Raimondo D, Andreotti G, Saint N, Amodeo P, Renzone G, Sanseverino M, Zocchi I, Molle G, Motta A, Scaloni A (2005) A folding-dependent mechanism of antimicrobial peptide resistance to degradation unveiled by solution structure of distinctin. Proc Natl Acad Sci USA 102:6309–6314

Rosenberger CM, Gallo RL, Finlay BB (2004) Interplay between antibacterial effectors: a macrophage antimicrobial peptide impairs *Salmonella* replication. Proc Natl Acad Sci USA 101:2422–2427

Sahl HG, Pag U, Bouness S, Wagner S, Antcheva N, Toss A (2005) Mammalian defensins: structures and mechanism of action. J Leukoc Biol 77:466–475

Sheu MJT, Baldwin WW, Brunson KW (1985) Cytotoxicity of rabbit macrophage peptides MCP-1 and MCP-2 for mouse tumor cells. Antimicrob Agents Chemother 28:626–629

Shaughnessy S, Nicholls P (1985) Control of respiration in sonicated cytochrome oxidase proteoliposomes by gated and ungated ionophores. Biochem Biophys Res Commun 128:1025–1030

Selsted ME, Ouelette AJ (2005) Mammalian defensins in the antimicrobial immune response. Nat Immunol 6:551–557

Seppet EK, Dhalla NS (1989) Characterization of Ca^{2+}-stimulated ATPase in rat heart sarcolemma in the presence of dithiothreitol and alamethicin. Mol Cell Biochem 19:137–147

Wong JH, Ng TB (2005) Sesquin, a potent defensin-like antimicrobial peptide from ground beans with inhibitory activities toward tumor cells and HIV-1 transcriptase. Peptides 26:1120–1126

Wroblewski H, Burlot R, Johansson KE (1978) Solubilization of *Spiroplasma citri* cell membrane proteins with the anionic detergent sodium lauroyl-sarcosinate (Sarkosyl). Biochimie 60:389–398

Yang L, Harroun TA, Weiss TM, Ding L, Huang HW (2001) Barrel-stave or toroidal model? A case study on melittin pores. Biophys J 81:1475–1485

Yonezawa A, Kuwahara J, Fujii N, Sugiura Y (1992) Binding of tachyplesin I to DNA revealed by footprinting analysis: significant contribution of secondary structure to DNA binding and implication for biological action. Biochemistry 31:2998–3004

Yount NY, Yeaman MR (2004) Multidimensional signatures in antimicrobial peptides. Proc Natl Acad USA 101:7363–7368

Zemel A, Ben-Shaul A, May S (2005) Perturbation of a lipid membrane by amphipathic peptides and its role in pore formation. Eur Biophys J 34:230–242

Zhang L, Rozek A, Hancock RE (2001) Interaction of cationic antimicrobial peptides with model membranes. J Biol Chem 276:35714–35722